PHYSICAL REVIEW E VOLUME 57, NUMBER 2 FEBRUARY 1998

Early-time dynamics of wave fronts in disordered triangular lattices

M. Kellomäki, J. Åström, and J. Timonen
Department of Physics, University of Jyväskylä, P.O. Box 35, FIN-40351 Jyväskylä, Finland
(Received 7 October 1997)

The early-time behavior of transient elastic wave fronts is analyzed in two-dimensional, randomly bond-diluted triangular lattices composed of Hooke springs. When the bond probability $p \simeq 1$, the wave-front amplitude first oscillates and then begins to decay algebraically. This power-law decay arises from dispersion. These phenomena should both be observable in, e.g., single cystals of fcc metals. For $p < 0.95$, the amplitude decay is caused by disorder and is exponential with a decay constant $\alpha \sim (1-p)^{1.7}$. There is a smooth crossover between these two types of behaviors. [S1063-651X(98)50702-7]

PACS number(s): 46.10.+z, 61.43.Bn, 62.30.+d, 63.20.−e

Basic features of pulse propagation in various linear and nonlinear media have long since been understood [1–3]. However, there are still many interesting new aspects [4,5], and novel applications of transient wave fronts [6], that are now emerging. Recently there has also been interest in disordered wave fronts [7] and phenomena in highly dispersive excitable media [8,9]. Most of the work published on classical waves in random media has dealt with long-time phenomena like localization and anomalous diffusion [10,11]. We have already shown [12,13] that there are interesting phenomena related also to the initial phases of a transient wave front propagating into two-dimensional random networks made of elastic beams or Hooke springs (micromechanical models of fibrous compounds). We found that, in addition to the ordinary elastic waves, the leading wave front also includes an exponentially decaying transient that propagates along independent one-dimensional paths made of beam segments. A similar transient was also found in diluted square lattices of elastic beams [14,15]. In this paper we report results for how *dispersion* and *disorder* of discrete networks contribute to the *early-time* dynamics of the leading front of elastic waves.

In Fig. 1 we show a bond-diluted triangular lattice with bond probability $p=0.9$. Two lattice directions, [10] and [11], are marked by arrows in this figure. This disordered network is made of massless Hooke springs (lattice constant a, spring constant K) and pointlike masses M (on lattice sites). We define the *wave-front velocity* (c.f. definitions in Refs. [1] and [16]) as the velocity of the first local displacement extremum and its *amplitude* as the absolute value of that extremum.

There are already many results [12–14] available for the wave-front velocity in similar networks. Here we consider the early-time behavior of the wave-front amplitude. Initially the network is at rest and no forces are present. A pulse is then induced in the network at $x=0$ of the form

$$f(t)=\begin{cases} A_S\cos(\omega_S t), & -\pi/2\omega_S \leqslant t \leqslant \pi/2\omega_S \\ 0, & \text{otherwise} \end{cases} \tag{1}$$

where A_S is the initial amplitude and ω_S the driving frequency. Fourier transform of the pulse at $x=0$ is denoted by $g(\omega,\omega_S)$, where ω is the frequency of the component wave. Notice that $g(\omega,\omega_S)$ has its global maximum at $\omega=0$ and oscillates symmetrically between positive and negative values as $|\omega|$ increases. We apply the stationary-phase method [1,2] in analyzing the time evolution of this pulse. Near the stationary values of the group velocity v_G, this method can be used to find the effective bandwidth $\Delta\omega$ of the wave group associated with v_G:

$$\Delta\omega(x)=\nu_M^{1/3}3^{1/3}v_G^{2/3}x^{-1/3}\left|\frac{d^2v_G}{d\omega^2}\right|^{-1/3}, \tag{2}$$

where ν_M is a dimensionless parameter describing the width of the wave group.

Let us first analyze the time evolution of a longitudinal pulse of form Eq. (1) in a perfect triangular network ($p=1$) in the case in which the pulse propagates in the [11] direction (a similar analysis can easily be done for other directions and polarizations). The dispersion relation of the network is in this case given by

$$k(\omega)=\begin{cases} \dfrac{4}{a\sqrt{3}}\arcsin\dfrac{\omega}{\omega_0\sqrt{6}}, & |\omega|\leqslant\omega_0\sqrt{6} \\ \dfrac{2\pi}{a\sqrt{3}}-i\dfrac{4}{a\sqrt{3}}\text{arcosh}\dfrac{\omega}{\omega_0\sqrt{6}}, & |\omega|>\omega_0\sqrt{6}, \end{cases} \tag{3}$$

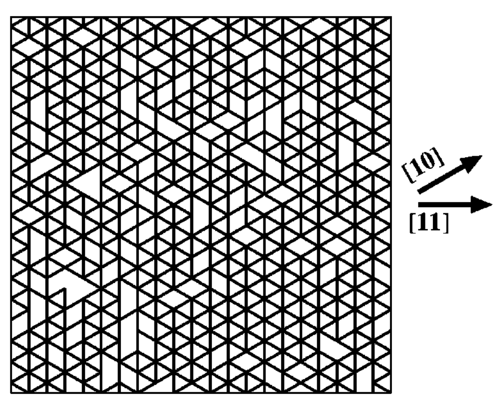

FIG. 1. Two-dimensional randomly bond-diluted triangular lattice ($p=0.90$). The arrows show the [10] and [11] directions in this lattice.

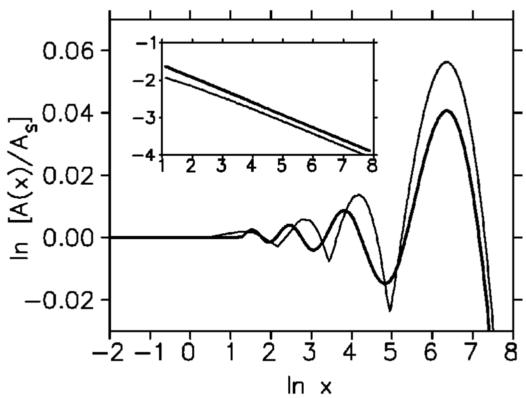

FIG. 2. Initial behavior of simulated (thin solid line) and calculated [bold solid line, Eq. (4)] wave-front amplitude A vs distance x in a perfect triangular lattice with $K=1.0$, $M=1.0$, $a=1.0$, and $\omega_S=0.15$. Inset shows the asymptotic behavior of the amplitude for $\omega_S=5.0$.

where $\omega_0:=\sqrt{K/M}$. The extrema of a wave train move with a local phase velocity $c(\omega)=\omega/k(\omega)$. Thus we find, in this case, that the first (the *fastest*) maximum must have the fastest phase velocity related to frequencies near $\omega=0$. Furthermore, $\omega=0$ is the point of global maximum in the group velocity $v_G(\omega)=d\omega/d[k(\omega)]$. This means that the components with $\omega\simeq 0$ form a stationary wave group. The dominant frequency [point of global maximum of $g(\omega,\omega_S)$] of the pulse is also $\omega=0$. We can thus conclude that the first maximum of the dispersed pulse is the biggest one, and that it belongs to a stationary wave group which travels with the highest group velocity $v_G(\omega=0)=c(\omega=0)=3/(2\sqrt{2})a\omega_0=:c$. The wave-front amplitude $A(x)$ can now be estimated by a simple sum of the component amplitudes $g(\omega,\omega_S)$ of the pulse Eq. (1) within the effective bandwidth given by Eq. (2) around $\omega=0$:

$$A(x)\propto\int_{-\Delta\omega(x)/2}^{\Delta\omega(x)/2} g(\omega,\omega_S)e^{-\alpha(\omega)x}d\omega, \tag{4}$$

where $\Delta\omega(x)=(16\nu_M)^{1/3}ca^{-2/3}x^{-1/3}$ and $\alpha(\omega)=\mathrm{Im}\{k(\omega)\}$. In the limit $x\to\infty$, the spectrum of the pulse behaves as $g(\omega,\omega_S)\approx A_S/(\pi\omega_S)$ within the band $\Delta\omega$, and this leads to an asymptotic power-law decay $A(x)\propto x^{-1/3}$.

For $p<1$ disorder is introduced in the network. As long as the wave front, initially started at $x=0$, has not encountered any missing bonds, its amplitude behaves as in the case $p=1$. Once it hits the first defect, it is locally (partly) reflected from the mechanically softer spot formed around a missing bond. The wave front loses some of its energy and its component structure (phase) is locally distorted. As it hits increasingly more defects, its phase coherence is finally destroyed, and its behavior changes. However, if p is close to unity, the dispersionlike behavior can last quite long. In our previous work [14] on the propagation of wave fronts in bond-diluted square lattices composed of elastic beams, we found that, if disorder is increased $(p<0.95)$, the wave-front amplitude A initially decays as $A(x)=A_0\exp(-\alpha x)$ with the decay constant α given by

$$\alpha=\alpha_0(1-p)^{\beta}, \quad \beta=1. \tag{5}$$

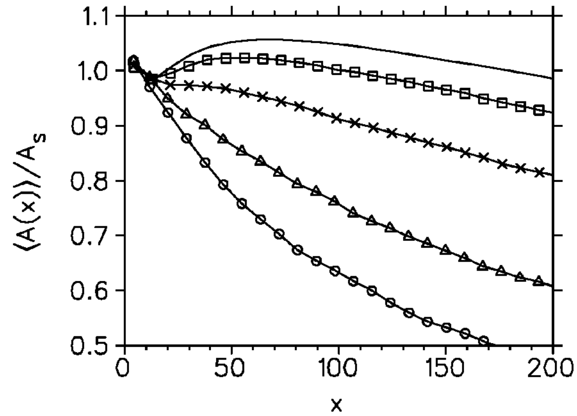

FIG. 4. Averaged data for the wave-front amplitude A as a function of distance x obtained from a simulation of 100×50 triangular lattices with $p=1.0$ (plain solid line), $p=0.997$ (boxes), $p=0.99$ (crosses), $p=0.97$ (triangles), and $p=0.95$ (circles). For each value of p the $A(x)$ curve was averaged over ten network samples. Other parameters were $K=M=a=1.0$, and $\omega_S=0.3$.

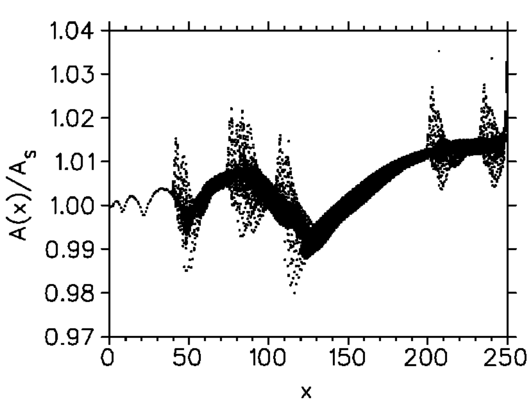

FIG. 3. Simulation data for the wave-front amplitude A as a function of distance x in a 1000×50 triangular lattice with $p=0.9999$. Other parameters were $K=M=a=1.0$, and $\omega_S=0.1$.

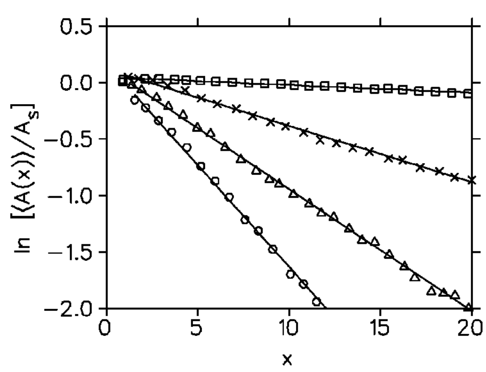

FIG. 5. Averaged initial wave-front amplitude A (in 100×50 lattices) vs distance x for $p=0.95$ (boxes), $p=0.80$ (crosses), $p=0.70$ (triangles), and $p=0.60$ (circles). For each value of p the $A(x)$ curve was averaged over 25 network samples. Other parameters were $K=M=a=1.0$, and $\omega_S=0.3$.

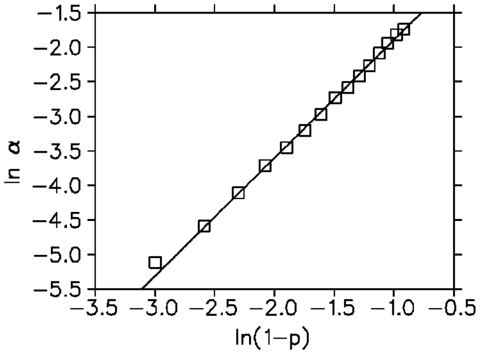

FIG. 6. Averaged initial decay constant α as a function of $1-p$ ($p=0.60,\ldots,0.95$, the other parameters as in Fig. 5).

In a triangular spring network considered here, a similar behavior could be expected. However, rigidity of a spring network is a nonlocal property (vector percolation), whereas it is a local property (scalar percolation) in a beam network. Therefore, missing bonds soften the spring network on a larger scale. The value of α is thus expected to grow as a function of $1-p$ more rapidly than in Eq. (5).

We have tested numerically the analytic results given above. The dynamics of the triangular network was directly computed using the velocity-Verlet (difference) method [17]. As expected, the first maximum was largest and was related to the lowest frequencies. In Fig. 2 we compare simulated (thin solid line) and calculated (bold solid line, numerical integration of Eq. (4) with ν_M as a free parameter: best fit gave $\nu_M \simeq 2.7$) wave-front amplitude $A(x)$ in the case $p=1$ ($K=1.0$, $M=1.0$, $a=1.0$, $\omega_S=0.15$). We notice that, for small x, $A(x)$ oscillates around the initial amplitude of the pulse. After the last oscillation, which is also largest, it begins to decay monotonically. It is evident from Fig. 2 that the number of oscillations, intervals between them, and their relative amplitudes, are satisfactorily described by Eq. (4). This equation tells how components with the highest frequencies are left behind the wave front as x increases. The amplitudes $g(\omega,\omega_S)$ of these components are alternately negative and positive which leads to the oscillating behavior of $A(x)$. The inset of Fig. 2 ($\omega_S=5.0$) confirms that the asymptotic power-law decay is correctly given by Eq. (4). It is noteworthy that the driving frequency ω_S sets the distance x_D, for a given lattice, after which the wave-front amplitude begins the monotonic decay. For small values of ω_S, the value of x_D can be very large. This behavior of the amplitude should be observable in, e.g., single monatomic fcc crystals in which dispersion relations similar to the two-dimensional case considered here appear. For a single crystal of lead, e.g., one can estimate from Eq. (2) that, in the [100] direction, the oscillating part of the wave-front amplitude will penetrate to a depth of $x_D=10$ mm, provided that the width of the positive part of the pulse spectrum is 130 GHz around $\omega=0$.

In Fig. 3 we show data simulated for the wave-front amplitude $A(x)$ in a 1000×50 network with $p=0.9999$ and $\omega_S=0.1$. For small values of x the amplitude oscillates just like in Fig. 2. At $x\simeq 40$ the wave front hits the first missing bond. The amplitude becomes immediately somewhat disturbed. One can observe how this defect, along with the other five missing bonds, give rise to local loss of phase coherence. In Fig. 4 we show the averaged amplitude $\langle A(x)\rangle$ for five different values of p ($\omega_S=0.3$). It is evident that the oscillating behavior caused by dispersion changes smoothly into immediate decay caused by disorder. The oscillating part of $\langle A(x)\rangle$ becomes shorter with decreasing p until all oscillations disappear. The early-time behavior of $\langle A(x)\rangle$ for $p=0.60,\ldots,0.95$ is shown in Fig. 5. It is obvious that for $p\leqslant 0.95$, the initial decay of $\langle A(x)\rangle$ is exponential. In Fig. 6 the initial decay constant α is plotted as a function of $1-p$. It is evident that the power-law form suggested by Eq. (5) applies also in this case. The best fit for the exponent gave $\beta=1.7$, which differs from $\beta=1$ found for the bond-diluted square lattices composed of elastic beams. It can be explained (c.f. above) why $\beta>1$ for spring networks, but the actual value of β is difficult to estimate analytically.

In conclusion, we have considered here the amplitude of the leading front of elastic waves in bond-diluted triangular lattices composed of equal springs and masses. We found that for $p\simeq 1$, the behavior of the wave-front amplitude is determined by dispersion. The driving frequency ω_S of the pulse sets the distance of the oscillating part of the wave-front amplitude. After this there is a power-law decay of the amplitude in the case $p=1$. As p is lowered below 0.95, the oscillating part vanishes and the amplitude decays exponentially right from the beginning. The decay constant was found to behave as $\alpha\sim(1-p)^{1.7}$ (valid when $p=0.60,\ldots,0.95$). The crossover from the dispersion-dominated ($p\simeq 1$) to the disorder-dominated ($p\leqslant 0.95$) behavior is smooth, and takes place within quite a narrow range of missing bond concentration $1-p$. A more comprehensive account of the dispersion, disorder and other mechanisms that affect the wave-front dynamics in various random discrete media will be given elsewhere [15].

[1] L. Brillouin, *Wave Propagation and Group Velocity* (Academic, New York, 1960).

[2] I. Tolstoy, *Wave Propagation* (McGraw-Hill, New York, 1973).

[3] A. Segel and G. H. Handelman, *Mathematics Applied to Continuum Mechanics* (Macmillan, New York, 1977).

[4] H. Wilhelmsson, J.-H. Trombert, and J.-F. Eloy, Phys. Scr. **52**, 102 (1995).

[5] C. M. Balictsis and K. E. Oughstun, Phys. Rev. E **55**, 1910 (1997).

[6] T.-T. Wu, J.-S. Fang, G.-Y. Liu, and M.-K. Kuo, J. Acoust. Soc. Am. **98**, 2142 (1995).

[7] M. Markus, T. Schulte, and A. Czajka, Phys. Rev. E **56**, R1 (1997).

[8] A. M. Pertsov, M. Wellner, and J. Jalife, Phys. Rev. Lett. **78**, 2656 (1997).

[9] M. Wellner and A. M. Pertsov, Phys. Rev. E **55**, 7656 (1997).

[10] *Scattering and Localization of Classical Waves in Random Media*, edited by P. Sheng (World Scientific, Singapore, 1990).

[11] P. Sheng, *Introduction to Wave Scattering, Localization, and Mesoscopic Phenomena* (Academic Press, New York, 1995).

[12] M. Kellomäki, J. Åström, and J. Timonen, Phys. Rev. Lett. **77**, 2730 (1996).

[13] J. Åström, M. Kellomäki, and J. Timonen, J. Phys. A **30**, 6601 (1997).

[14] J. Åström, M. Kellomäki, and J. Timonen, Phys Rev. E **56**, 6042 (1997).

[15] M. Kellomäki, J. Åström, and J. Timonen, Phys. Rev. E (to be published).

[16] J. L. Leander, J. Acoust. Soc. Am. **100**, 3503 (1996).

[17] D. W. Heermann, *Computer Simulation Methods in Theoretical Physics* (Springer-Verlag, Darmstadt, 1990).